A specialized niche in the pancreatic microenvironment promotes endocrine differentiation

Corinna Cozzitorto[1,2], Laura Mueller[1,3], Silvia Ruzittu[1,3], Nancy Mah[4], David Willnow[1,3], Jean-Francois Darrigrand[3], Heather Wilson[3], Daniel Khosravinia[3], Amir-Ala Mahmoud[5], Maurizio Risolino[5], Licia Selleri[5], Francesca M. Spagnoli[1,3,6*]

[1]Max-Delbrueck Center for Molecular Medicine, Robert-Roessle Strasse 10, Berlin 13125, Germany; [2]Department of Ophthalmology & Department of Anatomy, Institute for Human Genetics, University of California, San Francisco, CA 94143, USA; [3]Centre for Stem Cell and Regenerative Medicine, King's College London, Great Maze Pond, London SE1 9RT, United Kingdom; [4]Charité-Universitätsmedizin Berlin, 13353 Berlin, Germany; [5]Program in Craniofacial Biology, Institute for Human Genetics, Eli and Edythe Broad Center of Regeneration Medicine & Stem Cell Research, Department of Orofacial Sciences & Department of Anatomy, University of California, San Francisco, 513 Parnassus Ave, HSW 710, San Francisco, CA 94143, USA.

[6]Lead contact

Correspondence to: francesca.spagnoli@kcl.ac.uk

This PDF file includes:

Supplemental Figs. S1 to S6

Supplemental Table S1

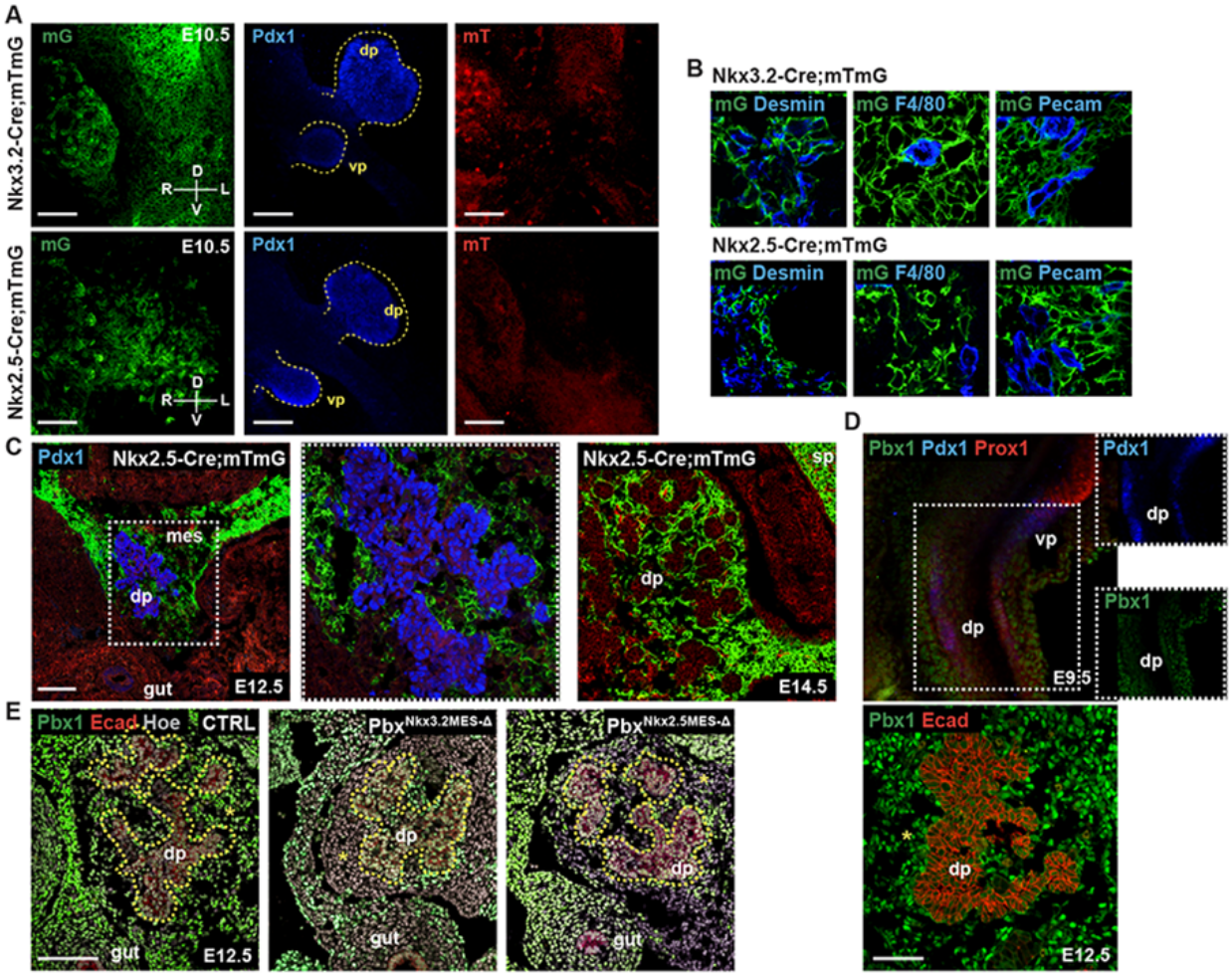

Figure S1. Nkx3.2- and Nkx2.5-mesenchymal domains surrounding the developing pancreas, Related to Figures 1 and 2. A, Single-channel maximum intensity z-projection images of whole-mount immunofluorescence (IF) staining for Pdx1 (blue) on E10.5 *Nkx3.2*- and *Nkx2.5-Cre;mTmG* embryos (related to Fig. 1B). Yellow dashed lines mark pancreatic buds; in green (mG), surrounding mesenchyme; in red (mT), non-recombined tissue. dp, dorsal pancreas; vp, ventral pancreas. $n = 3$ independent embryos of each genotype. Scale bars, 50 µm. **B,** Merged images of high magnification insets shown in Figures 1C and 1D. **C**, IF staining on cryosections of E12.5 and E14.5 *Nkx2.5-Cre;mTmG* embryos for the indicated markers. *Nkx2.5*-Cre-driven GFP (green) expression marks a subset of pancreatic mesenchymal cells. Boxed area is shown at higher magnification. $n = 3$ independent embryos were examined. Scale bar, 50 µm. **D**, Representative IF images of whole-mount E9.5 embryo and E12.5 pancreatic tissue cryosection stained for indicated markers. Insets show split channels Pbx1 (green) and Pdx1 (blue) of boxed area in E9.5 whole-mount IF. dp, dorsal pancreas; vp, ventral pancreas. *, marks the mesenchyme. Scale bar, 50 µm. **E**, IF analysis of Pbx1 and E-cadherin (Ecad) on control (CTRL), $Pbx^{Nkx2.5MES-\Delta}$ and $Pbx^{Nkx3.2MES-\Delta}$ E12.5 mouse pancreatic tissue cryosections. Absence of Pbx1 was visible in the mesenchyme (see *) of both $Pbx^{Nkx2.5MES-\Delta}$ and $Pbx^{Nkx3.2MES-\Delta}$ embryonic tissues. Hoechst (Hoe) was used as nuclear counterstain. Yellow dotted lines demarcate the pancreatic epithelium. dp, dorsal pancreas; mes, mesenchyme. Scale bar, 50 µm.

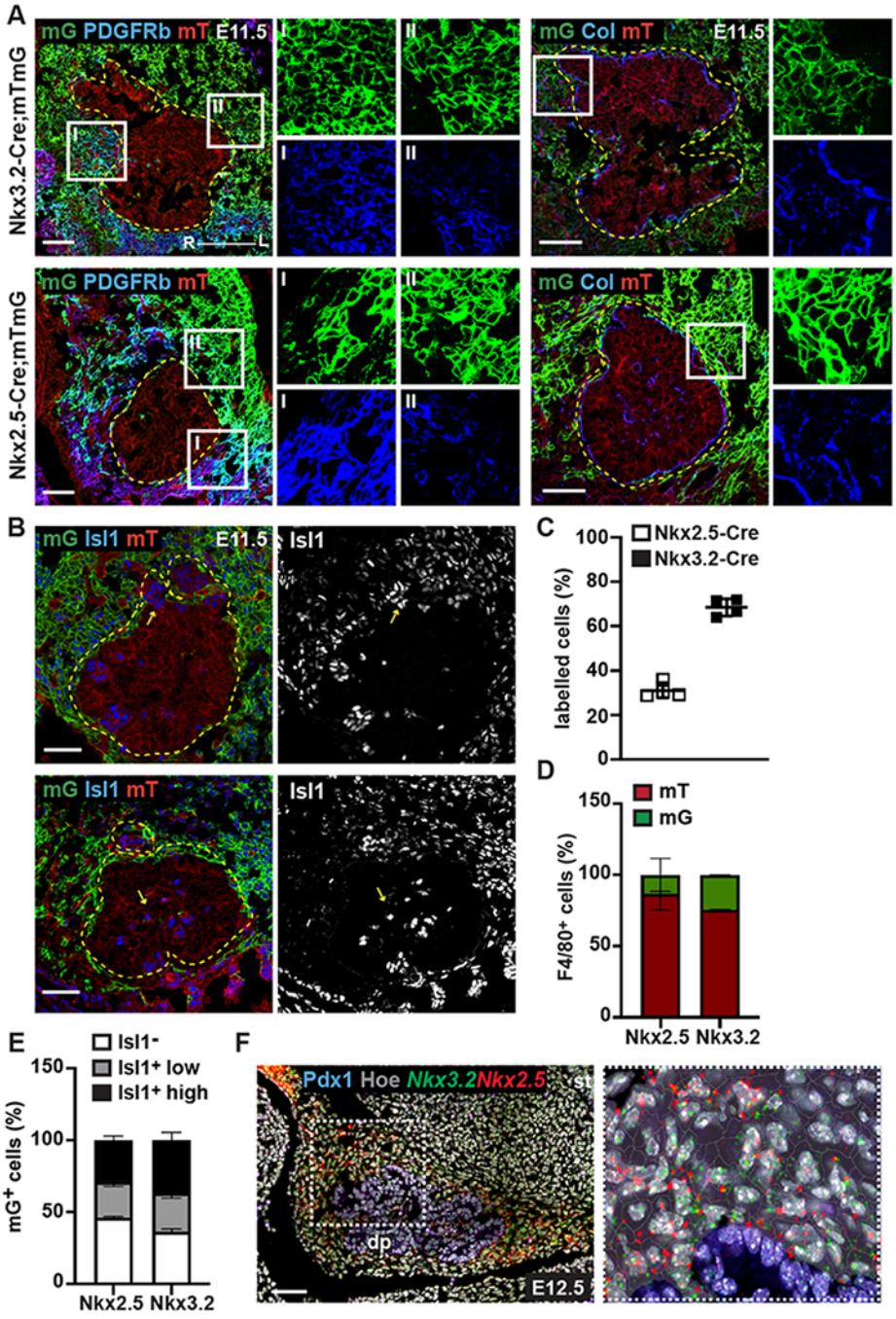

Figure S2. Colocalization of Nkx3.2- and Nkx2.5-descendant populations and mesenchymal markers, Related to Figure 1. A, Representative confocal images of IF staining on cryosections of E11.5 *Nkx3.2*- and *Nkx2.5-Cre;mTmG* embryos for the indicated markers. *Nkx2.5*-expressing cells (mG+, green) gave rise to a subset of pancreatic mesenchymal cells that are also positive for Collagen I (Col) and PDGFRβ. Collagen I is abundant in the interstitial matrix around the pancreatic mesenchyme. PDGFRβ marks multiple mesenchymal lineages in the embryo and becomes restricted to pericytes and vascular smooth muscle in adulthood (Harari et al. 2019). In the E11.5 pancreatic mesenchyme, PDGFRβ displayed a pattern of expression opposite to Nkx2.5-traced mesenchymal population, being mostly present on the right side of the dorsal

pancreas. Boxed areas are shown at higher magnification and as split channels on the right. Yellow dotted lines demarcate the pancreatic epithelium. Scale bar, 50 μm. **B**, Representative confocal images of IF staining for Islet-1 (Isl1) on cryosections of E11.5 *Nkx3.2*- and *Nkx2.5-Cre;mTmG* embryos. Consistently with previous reports, Isl1 was abundant in endocrine progenitors within the pancreatic epithelium (see arrows) as well as in the surrounding mesenchyme (Ahlgren et al. 1997). Yellow dotted lines demarcate the pancreatic epithelium. Scale bar, 50 μm. **C**, Quantification of Nkx3.2 (mG)- and Nkx2.5 (mG)-descendant cells in the spleno-pancreatic mesenchyme at E11.5. Cell segmentation was applied to IF stainings, the number of mG^+ (recombined) relative to the total of mT^+ (nonrecombined) cells was assessed in the region surrounding the dorsal pancreas (dp) and delimited by the mesothelium; the region surrounding stomach or duodenum was excluded from the analysis. Data are expressed as average percentage (%) ± s.d.. $n = 4$ independent embryos of each genotype. **D**, Quantification of Nkx3.2 (mG)- and Nkx2.5 (mG)-descendant cells that co-express the macrophage marker F4/80 in E11.5 pancreatic tissue cryosections (related to Figure 1C, 1D). Fluorescence intensity (FI) values for mTomato (mT) and mGFP (mG) were measured in $F4/80^+$ macrophage cells. 26.3% of $F4/80^+$ cells were mG^+ in *Nkx3.2-Cre;mTmG* embryos (n=562 cells); 9.8% of $F4/80^+$ cells were mG^+ in *Nkx2.5-Cre;mTmG* embryos (n=622 cells). **E**, Quantification of Isl1 levels in Nkx3.2 (mG)- and Nkx2.5 (mG)-descendant cells in E11.5 pancreatic tissue cryosections (shown in B). Isl1 FI was measured in Nkx3.2/mG^+ and Nkx2.5/mG^+ segmented cells on imaged cryosections of $n = 2$ independent embryos of each genotype. Results are expressed as average percentage (%) ± s.d.. **F**, Representative confocal images of RNAScope *in situ* hybridization for *Nkx2.5* (red) and *Nkx3.2* (green) mRNAs coupled with IF staining for Pdx1 (blue) on E12.5 pancreatic tissue cryosections. Inset shows magnified view of the area outlined by the dashed box. Hoechst nuclear counterstaining is shown in grey. dp, dorsal pancreas; st, stomach. Scale bar, 50 μm.

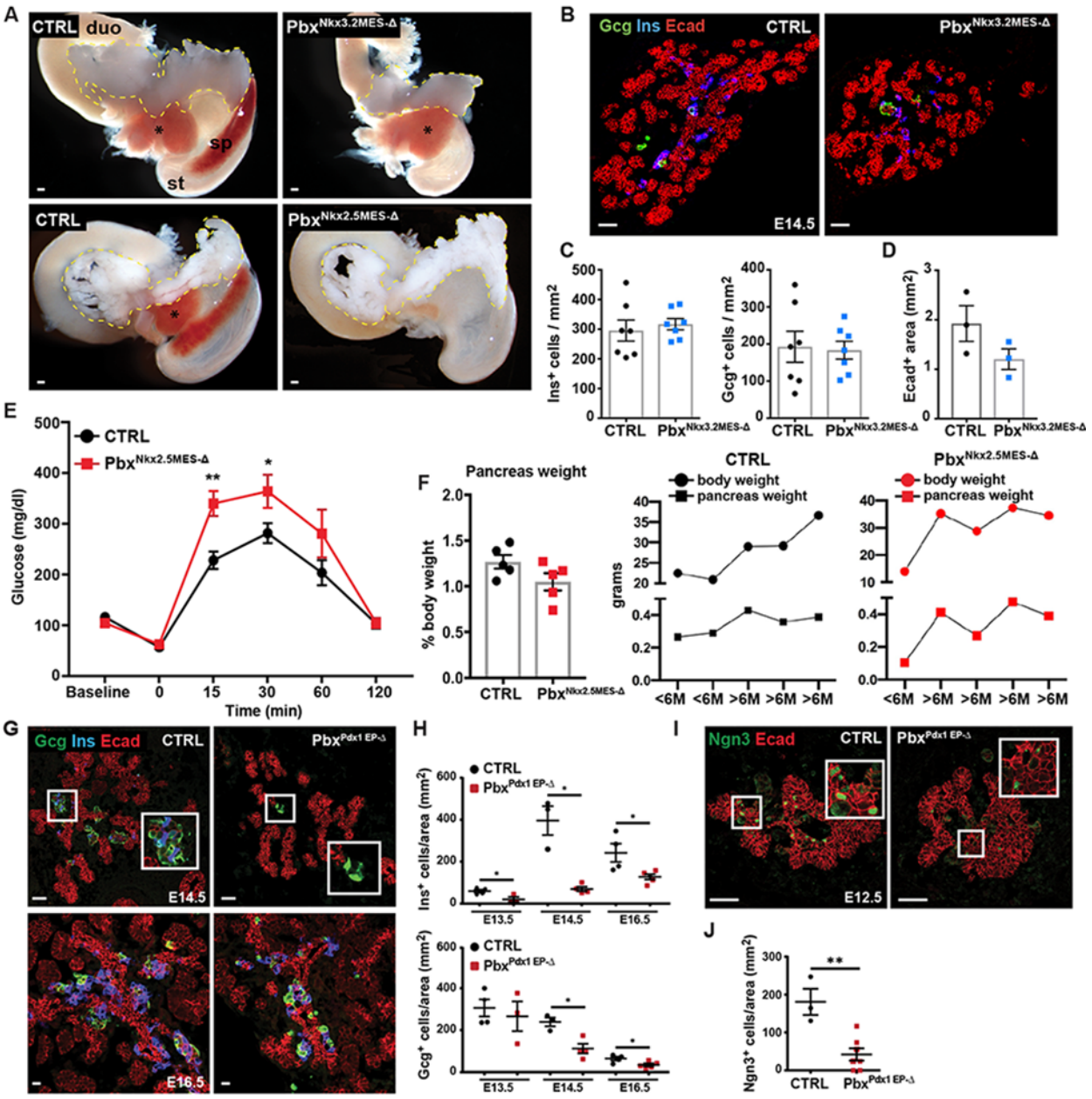

Figure S3. *Pbx1* deletion in distinct pancreatic populations, Related to Figures 2 and 3.

A, *Pbx1* was deleted in either Nkx3.2^{+} or Nkx2.5^{+} pancreatic mesenchymal populations. Gross morphology pictures of E18.5 control (CTRL), Pbx$^{Nkx2.5MES-\Delta}$ and Pbx$^{Nkx3.2MES-\Delta}$ pancreata. Yellow dotted lines mark the pancreata. Asterisks refer to residual pieces of liver lobes that were not dissected to ensure tissue integrity. duo, duodenum; sp, spleen; st, stomach. Scale bars, 200 µm. **B**, Representative IF images of E14.5 control (CTRL) and Pbx$^{Nkx3.2MES-\Delta}$ pancreata for Insulin (Ins), Glucagon (Gcg) and E-cadherin (Ecad). *Pbx1* was deleted in the whole foregut mesenchyme using the *Nkx3.2-Cre* mouse line (Pbx$^{Nkx3.2MES-\Delta}$). Ecad staining marks pancreatic epithelium. Scale bars, 50 µm. **C**, Quantification of the number of Insulin^{+} and Glucagon^{+} cells *versus* Ecad^{+} pancreatic area (mm^2) at E14.5. $n = 7$ independent embryos per genotype were examined. **D**, Measurement of pancreatic area on cryosections of CTRL and Pbx$^{Nkx3.2MES-\Delta}$ pancreata at E14.5. n=3 embryos per genotype were examined. **E**, GTT assay in adult mice (6-12

months age) showed that $Pbx^{Nkx2.5MES-\Delta}$ are glucose intolerant. Basal blood glucose (BG) level was measured before fasting the mice (baseline). After 16 hours of fasting, BG levels were measured before glucose injection (time 0) and subsequently at the indicated timepoints after glucose injection. n = 5 mice per group. *, $p<0.05$; **, $p<0.01$. **F**, Pancreas weight shown as a percent (%) of final body weight in $Pbx^{Nkx2.5MES-\Delta}$ and CTRL mice in adult age (left). Results are expressed as means ± s.e.m. n = 5 in each group. Right, plots showing the body and pancreas weight values of the individual CTRL and $Pbx^{Nkx2.5MES-\Delta}$ animals shown in F. min, minutes; M, months. **G-J,** *Pbx1* activity in the pancreatic epithelium. *Pbx1* was specifically deleted in the pancreatic epithelium through the use of *Pdx1-Cre* mouse transgenic line (Hingorani et al. 2003), in which the expression of the *Cre* recombinase is under the control of the *Pdx1* promoter (referred to as $Pbx^{EP-\Delta}$). Representative IF micrographs (G) and quantification of Insulin- and Glucagon-positive cells in CTRL and $Pbx^{EP-\Delta}$ embryos (H) at E13.5, E14.5 and E16.5. **I-J,** Quantification of Ngn3-positive cells in CTRL and $Pbx^{EP-\Delta}$ embryos at E12.5. The boxed areas are shown as a magnified views. Scale bars, 50 μm. $n \geq 3$ embryos per genotype were examined. Values shown are mean ± s.e.m. * $p<0.05$; ** $p<0.01$.

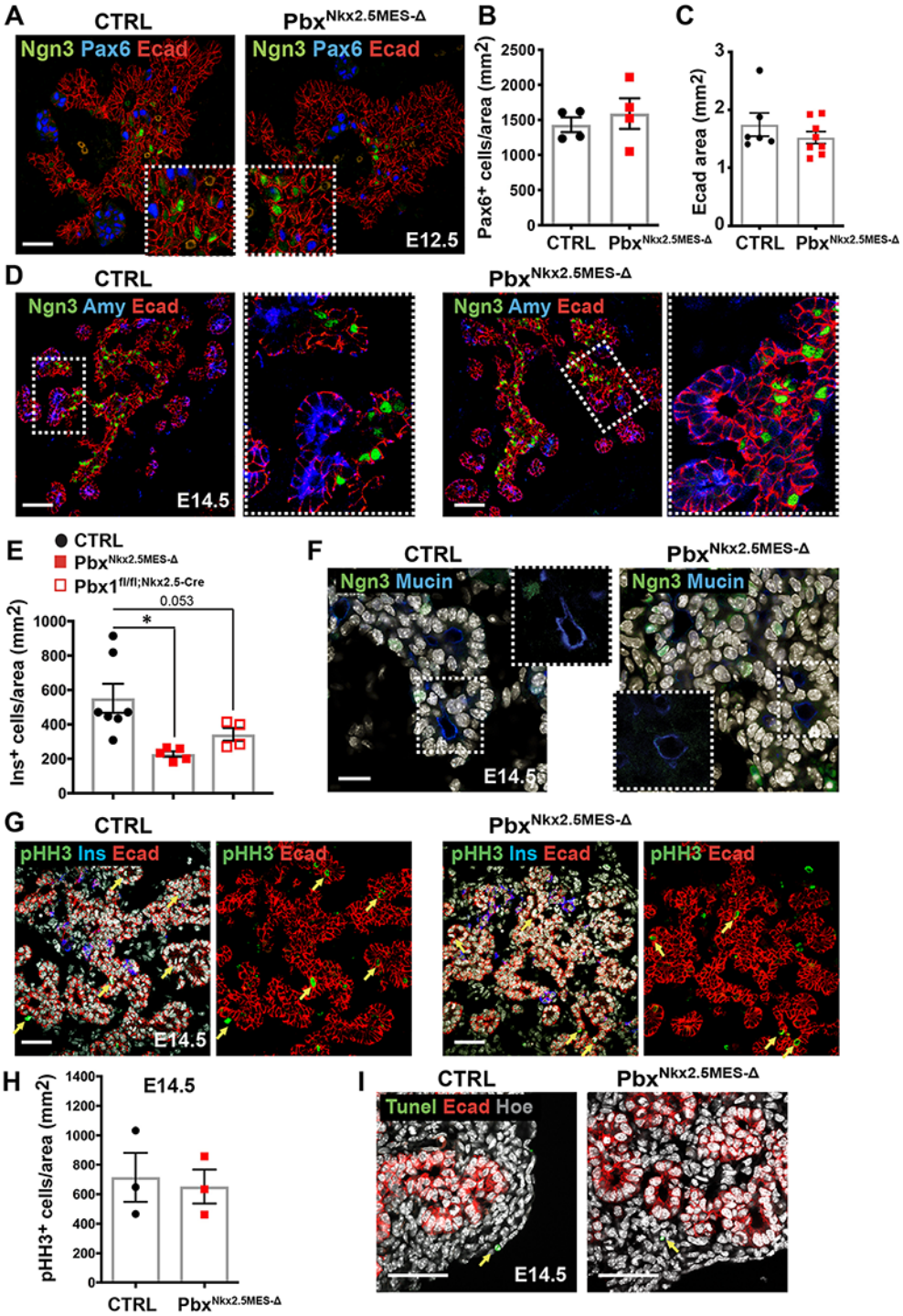

Figure S4. Characterization of pancreatic tissue upon deletion of *Pbx1* in the Nkx2.5 mesenchyme, Related to Figures 2 and 3. A, Representative images of Neurogenin3 (Ngn3), Pax6 and E-cadherin (Ecad) immunofluorescence (IF) on control (CTRL) and Pbx$^{Nkx2.5MES-\Delta}$ E12.5 mouse pancreatic cryosections. Scale bars, 50 µm. **B**, Quantification of the number of Pax6-positive (+) cells *versus* Ecad^{+} pancreatic area (mm^2) at E14.5. $n = 4$ independent embryos per genotype were examined. **C**, Measurement of pancreatic area on cryosections of CTRL and Pbx$^{Nkx2.5MES-\Delta}$ pancreata at E14.5. n=6 embryos (CTRL); n=8 embryos (Pbx$^{Nkx2.5MES-\Delta}$). **D,**

Representative IF micrographs of E14.5 control (CTRL) and $Pbx^{Nkx2.5MES-\Delta}$ pancreata for Amylase (Amy), Ngn3 and Ecad. Scale bars, 50 μm. Insets show boxed areas at higher magnification. *n* =3 embryos per genotype were examined. **E**, Quantification of $Insulin^{+}$ cells at E14.5 in single *Pbx1* ($Pbx1^{fl/fl;Nkx2.5}$) or compound *Pbx1*$^{fl/fl}$*;Pbx2*$^{+/-}$ ($Pbx^{Nkx2.5MES-\Delta}$) mutant embryos. Cell counts were normalized to the $Ecad^{+}$ pancreatic epithelium area (mm^2). n=7 embryos (CTRL); n=5 embryos ($Pbx^{Nkx2.5MES-\Delta}$); n=4 embryos ($Pbx1^{fl/fl;Nkx2.5}$) were examined. * $p<0.05$. **F,** Representative IF micrographs of E14.5 control (CTRL) and $Pbx^{Nkx2.5MES-\Delta}$ pancreata for Mucin and Ngn3. Hoechst (gray) was used as nuclear counterstain. Insets show boxed area at higher magnification. Scale bar, 20 μm. **G**, Representative IF micrographs of the mitosis marker Phosho-Histone H3 (pHH3), Insulin (Ins) and Ecad on E14.5 control (CTRL) and $Pbx^{Nkx2.5MES-\Delta}$ pancreata. Hoechst nuclear counterstaining is shown in grey. Right panels, pHH3 and Ecad signal channels only. Arrows indicate $pHH3^{+}$ nuclei in the epithelium. Scale bars, 50 μm. **H,** Quantification of $pHH3^{+}$ cells on cryosections of E14.5 CTRL and $Pbx^{Nkx2.5MES-\Delta}$ pancreata. Cell numbers were measured and normalized to the area (in mm2) of the $Ecad^{+}$ pancreatic epithelium. *n* =3 embryos per genotype were examined. **I,** Representative IF of TUNEL assay performed on cryosections of E14.5 CTRL and $Pbx^{Nkx2.5MES-\Delta}$. Arrows indicate TUNEL-positive nuclei in the mesenchyme. Experiments were repeated at least 3 times with similar results. Scale bars, 50 μm.

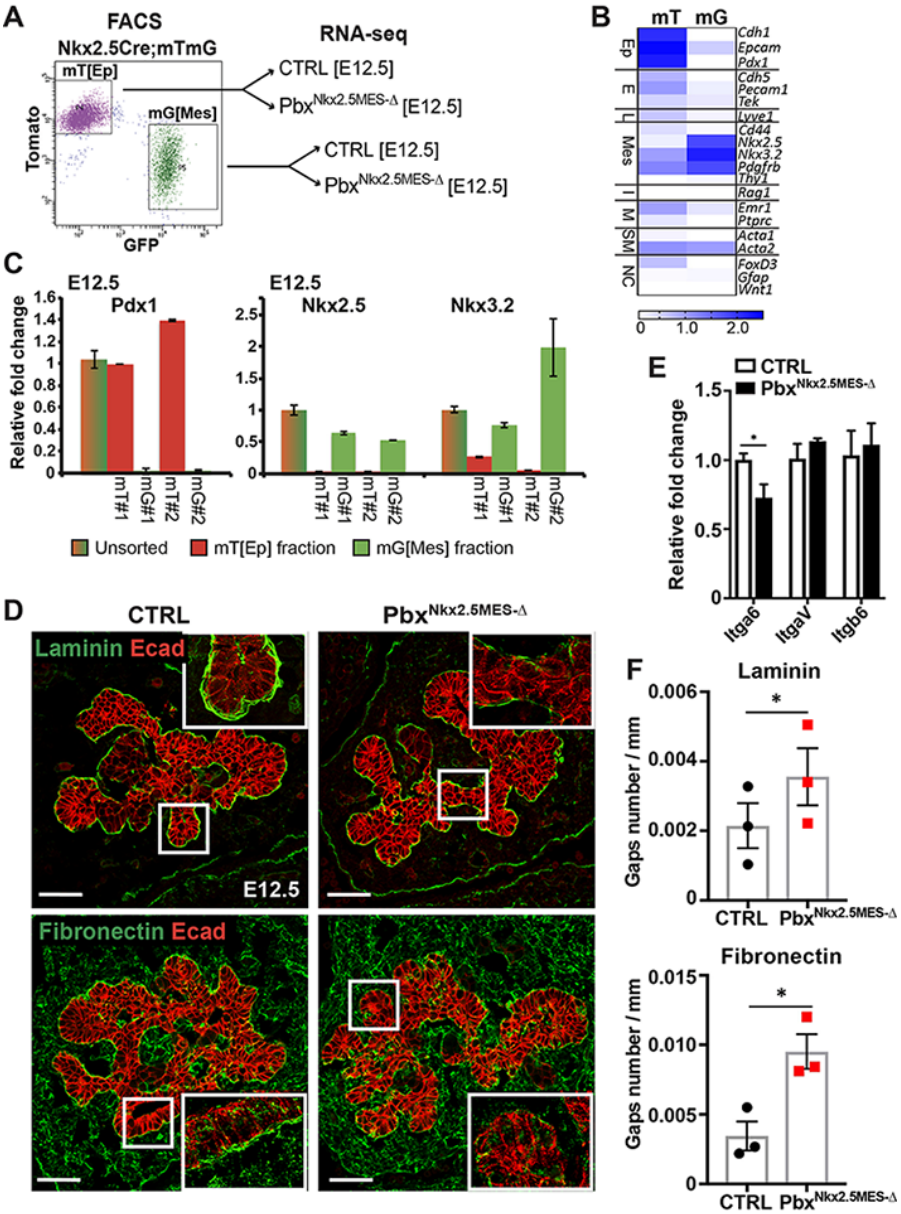

Figure S5. Characterization of Pbx-dependent regulatory networks in the Nkx2.5^{+} pancreatic mesenchyme, Related to Figures 4 and 5. A, Representative profile of FACS-sorted mT^{+} and mG^{+} fractions from *Nkx2.5*-Cre;mTmG (CTRL) and mTmG;Pbx$^{Nkx2.5MES-\Delta}$ (MUT) pancreata. RNA-Seq was performed on the indicated populations. **B**, Heatmap illustrates well-known lineage-specific markers, including epithelial /pancreatic (Ep), endothelial (E), lymphatic (L), mesenchymal (Mes), immune (I), macrophage (M), smooth-muscle (SM) and neural crest (NC) genes, in the FACS-sorted mT^{+} and mG^{+} fractions. Colors represent high (blue) or low (white) expression values based log 10 of the FPKM values for each gene. **C**, Representative RT-qPCR analysis of indicated marker genes on FACS-sorted mT^{+} and mG^{+} fractions from E12.5 mTmG pancreata and unsorted controls. As expected, *Pdx1* was exclusively expressed in the mT fraction, therefore referred to as epithelial [Ep]. By contrast, the mesenchymal TFs *Nkx2.5* and *Nkx3.2* were enriched in the mG/mesenchymal [Mes] fraction. Low level of *Nkx3.2* expression was detected in one of the mT[Ep] fractions, possibly

representing the contribution of non-lineage traced surrounding cells. Unsorted cells were used as positive control of the RT-qPCR assay. mT and mG fractions were collected in duplicate, each bar represents an independent biological replicate. Data are shown as mean ± s.e.m. of expression values relative to unsorted samples normalized on *36B4* expression. **D**, Representative IF micrographs of Laminin and Fibronectin on E12.5 control (CTRL) and $Pbx^{Nkx2.5MES-\Delta}$ pancreatic tissue. Boxed areas are shown as a magnified view, displaying a fragmented basement membrane (BM) in mutant embryos. Scale bars, 50 μm. **E**, RT-qPCR validation analysis of indicated Integrin genes on epithelial fractions derived from CTRL and MUT embryos. Data are represented as relative fold change normalized on *36B4* expression. Values shown are mean ± s.e.m. $n \geq 3$. * $p<0.05$. Statistical significance was calculated using two-tailed Student's *t*-test. **F**, Measurement analysis of gap numbers in Laminin- and Fibronectin-positive BM on E12.5 control (CTRL) and $Pbx^{Nkx2.5MES-\Delta}$ pancreatic tissue. Regions of the epithelium immediately adjacent to the BM lacking Laminin or Fibronectin immunoreactivity were measured and shown as ratio to the total BM perimeter (mm). $n = 3$ embryos per genotype were examined. * $p<0.05$.

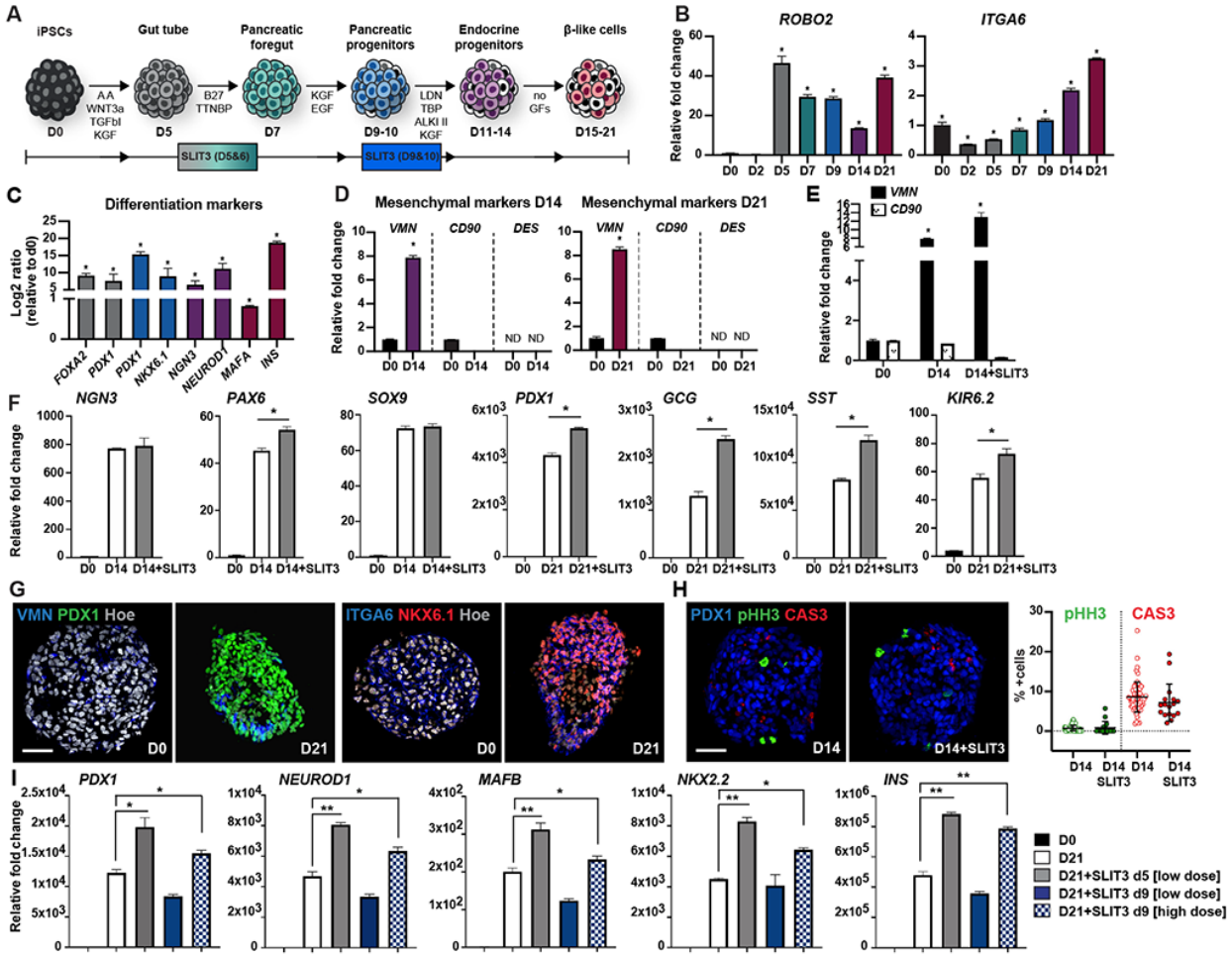

Figure S6. SLIT3 treatment promotes endocrine differentiation in human iPSCs without influencing cell proliferation or death, Related to Figure 6. A, Schematic representation of the differentiation protocol of iPSCs into β-like cells (Russ et al., 2015). Cell clusters were treated in suspension with SLIT3 for 48h at day (D) 5 of differentiation or at D9 of differentiation. **B**, RT-qPCR analysis of indicated stage-specific markers. Values were normalized to glyceraldehyde 3-phosphate dehydrogenase (*GAPDH*) and shown as Log2 ratio relative to day 0. **C**, RT-qPCR analyses of indicated marker genes in undifferentiated iPSCs (D0) and cells at subsequent steps of differentiation. Data are represented as relative fold change compared to D0. **D**, RT-qPCR analyses of indicated mesenchymal marker genes in undifferentiated iPSCs (D0) and cells at D14 and D21 of differentiation. Data are represented as relative fold change. Values shown are mean ± s.e.m. n=3 independent differentiation experiments. * p <0.05. Statistical significance was calculated using two-tailed Student's *t*-test. **E**, RT-qPCR analyses of indicated mesenchymal marker genes in undifferentiated iPSCs (D0) and differentiated cells cultured in presence of SLIT3 recombinant protein or left untreated. *VIMENTIN* (*VMN*) is expressed in iPSCs before differentiation and its level of expression modestly increased during differentiation. Further induction of mesenchymal markers or expansion of mesenchymal cells was not observed upon SLIT3 treatment. Data are represented as relative fold change compared to D0. Values shown are mean ± s.e.m. n=3 independent differentiation experiments. * p <0.05; two-tailed Student's *t*-test. **F**, RT-qPCR analysis of

selected gene transcripts in undifferentiated iPSCs (D0) and differentiated cells at D14 and D21 cultured with SLIT3 recombinant protein or untreated. Data are represented as relative fold change compared to D0. Values shown are mean ± s.e.m. * $p<0.05$; two-tailed Student's *t*-test. **G**, Representative IF images of differentiated clusters at D21 for the indicated markers. INTEGRIN-α6 (ITGA6) is present in undifferentiated D0 iPSCs and continues to be expressed throughout differentiation. Hoechst (Hoe) was used as nuclear counterstain. Scale bars, 50 um. **H**, Representative IF images of the mitosis marker Phospho-histone H3 (pHH3) and apoptotic marker Caspase 3 (CAS3) in differentiated clusters at D14 upon treatment with SLIT3 or left untreated. Scale bars, 50 um. Scatter plot shows no changes in $pHH3^+$ or $Cas3^+$ cells upon treatment of cell clusters with SLIT3. The number of $pHH3^+$ and $Cas3^+$ cells was normalized to the total number of cells contained in each cluster and shown as %. n=3 independent differentiation experiments. **I**, RT-qPCR analysis of selected gene transcripts in undifferentiated iPSCs (D0), D21 untreated control and treated with SLIT3 at D5 or at D9 of differentiation with low [100ng/ml] or high [500ng/ml] doses of recombinant protein. D5 SLIT3 treatment is most effective; cells respond to late time-point (D9) SLIT3 treatment only when stimulated at higher doses. This is in line with the level of expression of *ROBO2* receptor being higher at D5 than at D9 and suggests a dose dependent effect of SLIT3 in differentiating stem cell clusters. Data are represented as relative fold change compared to D0. Values shown are mean ± s.e.m. * $p<0.05$; ** $p<0.01$; two-tailed Student's *t*-test.

Table S1. Bulk RNA-Seq Analysis, Related to Figure 4.

Embryonic day & cell type	Genotype	Mapped reads	Annotated transcripts
E12.5 mT [epithelium]	CTRL	53,843.812	15,371
	MUT	40,102.738	15,201
E12.5 mG [mesenchyme]	CTRL	39,675.980	14,171
	MUT	42,217.024	14,167

Notes. CTRL, *Nkx2.5-Cre;mT/mG*; MUT, *Nkx2.5-Cre;mT/mG;Pbx1$^{flox/flox}$;Pbx2$^{+/-}$* (Pbx$^{Nkx2.5MES-\Delta}$). RNA was extracted from multiple embryos pooled together (≥4 controls and Pbx$^{Nkx2.5MES-\Delta}$) and, subsequently, processed for RNA-seq. A comparable number of high-quality raw reads was obtained from each sample and used to estimate the relative abundance of transcripts. An average of 14,000 annotated distinct transcripts per sample was detected. An absolute value of log2(FC) > 0.5 was chosen as a cut-off for differential expression.